

Automated tube voltage selection for radiation dose and contrast medium reduction at coronary CT angiography using 3rd generation dual-source CT

Stefanie Mangold^{1,2} · Julian L. Wichmann^{1,3} · U. Joseph Schoepf^{1,4} · Zachary B. Poole¹ · Christian Canstein⁵ · Akos Varga-Szemes¹ · Damiano Caruso^{1,6} · Fabian Bamberg² · Konstantin Nikolaou² · Carlo N. De Cecco¹

Received: 13 November 2015 / Revised: 9 December 2015 / Accepted: 22 December 2015 / Published online: 4 February 2016
© European Society of Radiology 2016

Abstract

Objectives To investigate the relationship between automated tube voltage selection (ATVS) and body mass index (BMI) and its effect on image quality and radiation dose of coronary CT angiography (CCTA).

Methods We evaluated 272 patients who underwent CCTA with 3rd generation dual-source CT (DSCT). Prospectively ECG-triggered spiral acquisition was performed with automated tube current selection and advanced iterative reconstruction. Tube voltages were selected by ATVS (70–120 kV). BMI, effective dose (ED), and vascular attenuation in the coronary arteries were recorded. Signal-to-noise ratio (SNR) and contrast-to-noise ratio (CNR) were calculated.

Five-point scales were used for subjective image quality analysis.

Results Image quality was rated good to excellent in 98.9 % of examinations without significant differences for proximal and distal attenuation (all $p \geq .0516$), whereas image noise was rated significantly higher at 70 kV compared to ≥ 100 kV (all $p < .0266$). However, no significant differences were observed in SNR or CNR at 70–120 kV (all $p \geq .0829$). Mean ED at 70–120 kV was 1.5 ± 1.2 mSv, 2.4 ± 1.5 mSv, 3.6 ± 2.7 mSv, 5.9 ± 4.0 mSv, 7.9 ± 4.2 mSv, and 10.7 ± 4.1 mSv, respectively (all $p \leq .0414$). Correlation analysis showed a moderate association between tube voltage and BMI ($r = .639$).

Conclusion ATVS allows individual tube voltage adaptation for CCTA performed with 3rd generation DSCT, resulting in significantly decreased radiation exposure while maintaining image quality.

Key Points

- Automated tube voltage selection allows an individual tube voltage adaption in CCTA.
- A tube voltage-based reduction of contrast medium volume is feasible.
- Image quality was maintained while radiation exposure was significantly decreased.
- A moderate association between tube voltage and body mass index was found.

Electronic supplementary material The online version of this article (doi:10.1007/s00330-015-4191-4) contains supplementary material, which is available to authorized users.

✉ U. Joseph Schoepf
schoepf@musc.edu

¹ Division of Cardiovascular Imaging, Department of Radiology and Radiological Science, Medical University of South Carolina, Charleston, SC, USA

² Department of Diagnostic and Interventional Radiology, Eberhard-Karls University Tuebingen, Tuebingen, Germany

³ Department of Diagnostic and Interventional Radiology, University Hospital Frankfurt, Frankfurt, Germany

⁴ Division of Cardiology, Department of Medicine, Medical University of South Carolina, Charleston, SC, USA

⁵ Siemens Medical Solutions, Malvern, PA, USA

⁶ Department of Radiological Sciences, Oncology and Pathology, University of Rome “Sapienza”, Rome, Italy

Keywords Coronary CT angiography · Automated tube voltage selection · Image quality · Body mass index · Radiation dose reduction

Abbreviations

ATVS Automated tube-voltage selection
CCTA Coronary CT angiography

CI	Confidence interval
CNR	Contrast-to-noise ratio
DSCT	Dual-source CT
SNR	Signal-to-noise ratio
SSDE	Size-specific dose estimates

Introduction

As the use of coronary CT angiography (CCTA) has grown, numerous technical advances have been implemented to decrease radiation dose without impacting image quality. Many efforts have been undertaken to individually tailor CT protocols to patient-specific characteristics. In this context, tube-voltage reduction has been shown to simultaneously enhance vascular signal and reduce radiation exposure at CTA [1–6]. A fully-automated voltage selection (ATVS) algorithm is available, which uses an individual patient's attenuation profile as determined by the planning ("scout") scan and information on the type of examination to custom-tailor the tube potential.

The potential of this ATVS algorithm to reduce radiation dose has been previously described [7–15]. Significant radiation dose reduction with maintained or even improved image quality has been reported for CCTA performed with a second generation DSCT system using ATVS compared to body mass index (BMI)-based tube-voltage selection [12, 14]. Improved image quality and lower radiation dose was also observed for third generation DSCT ATVS, which selects tube voltages ranging from 70–150 kV at 10 kV-increments, when compared to standard imaging protocols with fixed tube voltages [7, 13].

The purpose of our study was to assess the radiation dose and image quality of CCTA studies performed with third generation DSCT and ATVS in order to evaluate the efficiency of the automated algorithm at each tube voltage, and to investigate the impact of BMI on tube voltage selection and radiation dose.

Materials and methods

Patient population

This retrospective study was approved by the local Institutional Review Board with a waiver of informed consent.

We identified 280 patients who had undergone CCTA on a third generation DSCT system between May 2014 and September 2015. Patients were excluded if severe metal or motion artefacts were present, ECG synchronization was compromised, the patient was unable to elevate the arms over the head, or if any deviations from the standard scan protocol had occurred. Indications for CCTA included acute chest pain ($n=179$) and atypical chest pain ($n=47$). The remaining patients ($n=46$) were asymptomatic and examinations were performed within the framework of preoperative risk

stratification for potential liver transplant surgery ($n=7$), mitral valve replacement ($n=17$), and aortic valve replacement ($n=14$), as well as postoperatively in cases of heart transplantation ($n=3$) and aortic aneurysm repair ($n=5$).

CT acquisition parameters

All examinations were performed with a third generation DSCT system (SOMATOM Force, Siemens Healthcare, Forchheim, Germany) equipped with a fully integrated circuit detector system (Stellar Infinity, Siemens) and two x-ray tubes (Vectron, Siemens) with substantially increased power (120 kW each) enabling tube currents to reach up to 1300 mAs and, thus, allowing for low-kV studies to be performed within a broader patient collective [16]. A prospectively ECG-triggered adaptive sequential-mode acquisition protocol was used, which acquires images at 20 % of the nominal tube current between 30–90 % of the RR interval and full nominal tube current at 40 % or 70 % of the cardiac cycle, depending on the heart rate. The scan length for CCTA ranged from the carina to the cardiac apex. All studies were performed using automated tube current modulation (CARE Dose4D, Siemens) and ATVS (CARE kV, Siemens) with tube voltage settings ranging from 70 to 120 kV in 10 kV increments.

Further scan parameters were as follows: adaptive detector collimation varying from 96–192 in increments of 8×0.6 mm, gantry rotation of 0.25 s, and a pitch of 1.0.

Vessel attenuation was achieved using intravenously administered iodinated contrast agent (350 mgI/mL iohexol, Omnipaque, General Electric, Chalfont St. Giles, UK) at a flow rate of 4.5 mL/s, followed by a 50 mL saline chaser injected at the same flow rate. Contrast medium volume was adapted to the tube voltage (70 kV, 50 mL; 80 kV, 60 mL; 90 kV, 70 mL; ≥ 100 kV, 80 mL) based on our standard clinical protocols derived from prior studies on individual injection protocol adaptations and attenuation changes at different tube voltages [1, 16].

Using bolus-tracking software (CARE Bolus, Siemens), a region of interest (ROI) was placed within the descending aorta at the level of the carina and the scan was started automatically 4 seconds after a threshold of 100 Hounsfield units (HU) was reached [7].

Image reconstruction

All studies were reconstructed with dedicated third generation advanced modeled iterative reconstruction (ADMIRE, Siemens) at a strength level of 3 using a medium sharp convolution kernel (Bv36), 0.6 mm section thickness, and an increment of 0.4 mm. The reconstruction phase that provided the best image quality while minimizing motion artefacts (BestPhase, Siemens) was chosen for the analysis.

Objective image quality analysis

Attenuation was measured by drawing ROIs in the major coronary arteries (left main [LM], left anterior descending [LAD], circumflex [CX], and right coronary artery [RCA]), which were scaled as largely as possible (average size, 10 mm²). Vessel walls, calcifications, non-calcified plaque, and stented segments were all carefully avoided. LAD, CX, and RCA measurements were determined within the first 5 mm of the proximal and distal vessel segment as defined by the standard American Heart Association segmentation model [17]. Image noise was defined as the standard deviation (SD) of CT measurements of a ROI (size, 2 cm²) in the left ventricular blood pool. CT attenuation of the pericardial fat tissue adjacent to the vessel contour was measured in order to determine vessel contrast.

Signal-to-noise ratio (SNR) and contrast-to-noise ratio (CNR) were calculated for each measurement as previously proposed [18]:

$$\text{SNR} = (\text{CT attenuation}_{\text{proximal or distal coronary arteries}} / \text{noise})$$

$$\text{CNR} = ((\text{CT attenuation}_{\text{proximal or distal coronary arteries}} - \text{CT attenuation}_{\text{fat}}) / \text{noise})$$

Subjective image quality analysis

Dedicated post-processing and evaluation software (syngo.via VA30, Siemens) was used for both objective and subjective analysis.

Subjective image quality was assessed by two readers with 6 (S.M.) and 2 years (Z.B.P.) of cardiovascular imaging experience. Reviewers were blinded to the clinical indication for imaging, patient characteristics, and the clinical imaging report. The studies were interpreted individually and in random order. Window settings were freely adjustable. The contrast attenuation in the major coronary artery segments (LM, proximal and distal LAD, CX, and RCA) and the severity of image noise were graded using a modified scoring system as previously described [19]: vessel attenuation was defined as: 1 = poor opacification, insufficient for diagnosis; 2 = suboptimal opacification, low diagnostic confidence; 3 = acceptable opacification of major coronary arteries, sufficient for diagnosis; 4 = good opacification of proximal and distal segments; and 5 = excellent opacification of proximal and distal segments. The accompanying image noise was rated using a 5-point scale defined as: 1 = major noise, not acceptable for diagnosis; 2 = major noise, suboptimal evaluation with low confidence; 3 = moderate noise, sufficient for diagnosis; 4 = minor noise, diagnosis not influenced; and 5 = none perceivable. Image quality was classified as sufficient for diagnosis if both vessel opacification and noise were rated as ≥ 3 . In case of disagreements between readers regarding diagnostic image quality (i.e., a score of ≥ 3 by one reviewer and < 3 by the second reviewer), scores were arbitrated by a third observer with > 15 years of cardiovascular imaging experience (U.J.S.).

Radiation dose

Patient BMI was recorded and lateral and anteroposterior chest diameters were measured on scout and axial images. The effective chest diameter was calculated as the square root of the product of both chest diameter measurements [20].

The volume CT dose index (CTDI_{vol}; 32 cm phantom), effective tube current, and dose-length-product (DLP) were recorded for each examination. Effective radiation dose was estimated by multiplying the DLP with a standard conversion factor of 0.014 mSv/mGy*cm [21].

Furthermore, to correct for patient sizes deviating from the 32 cm phantom, size-specific dose estimates (SSDE) were calculated by multiplying the CTDI_{vol} with an effective diameter-based, size-specific conversion factor for a 32 cm phantom [22].

Statistical analysis

Commercially available software (MedCalc Statistical Software, v12.7.5.0, MedCalc bvba, Ostend, Belgium) was used for statistical analysis. Mean and SD were calculated for all numerical results derived from multiple measurements. The Kolmogorov-Smirnov test was used to test for normal distribution, and a *p*-value < 0.05 was considered statistically significant.

Differences in patient characteristics, objective image quality (vessel attenuation, image noise, SNR and CNR), and radiation dose estimates were tested between the different tube voltages by using the *t*-test for independent samples.

In order to compare subjective image quality, the mean score averaged from the two readers was evaluated using the Mann-Whitney U test. Spearman's correlation coefficient was calculated to examine possible correlation between effective chest diameter and BMI, as well as to calculate the influence BMI and effective chest diameter have on tube voltage selection. BMI-based thresholds for tube voltage selection were defined using 95 % confidence intervals (CI) of the mean BMI that were calculated for each tube voltage.

Inter-rater agreement was analyzed with Cohen's kappa (κ) analysis. Coefficients were interpreted in the following manner: $\kappa < 0.20$ = slight agreement, $\kappa: 0.21 - 0.40$ = fair agreement, $\kappa: 0.41 - 0.60$ = moderate agreement, $\kappa: 0.61 - 0.80$ = good agreement, and $\kappa: 0.81 - 1.0$ = excellent agreement.

Results

Patient population

Of the 280 patients initially identified, we excluded a total of eight patients who were unable to elevate the arms over the head ($n = 6$), or compromised ECG-synchronization ($n = 2$). Thus, a total of 272 patients who had undergone CCTA were included. Overall, our study cohort had a mean age of

56.9±15.1 years, a mean BMI of 29.4±7.0 kg/m², and was comprised of 148 women (mean age, 57.5±15.0 years; mean BMI, 30.5±8.1 kg/m²) and 134 men (mean age, 56.2±15.1 years; mean BMI, 28.3±5.7 kg/m²; *p* = .4905 and .0123, respectively). Mean heart rate was 68.5±14.3 beats per minute (bpm, women: 70.2±16.3 bpm; men: 68.7±16.6 bpm, *p* = .8652) and no significant differences were found between the heart rates at each tube voltage (*p*-values between .0740 and .6223). Detailed patient specific data are summarized in Table 1.

A total of 1884 coronary artery attenuation measurements were performed, but ten coronary arteries in eight patients were excluded due to severe calcifications (*n* = 6) or motion artefacts (*n* = 4).

Tube voltage selection and radiation dose

Detailed radiation dose data are shown in Table 2. A continuous increase in radiation dose was observed for all 10 kV increments in the 70 to 120 kV range. Significant differences were noted between 70 and 80 kV (CTDI, *p* = .0053; DLP, *p* = .0063; SSDE, *p* = .0090; ED, *p* = .0064), 80 and 90 kV (CTDI, *p* = .0430; DLP, *p* = .0462; SSDE, *p* = .0270; ED, *p* = .0334), 90 and 100 kV (CTDI, *p* = .0099; DLP, *p* = .0006; SSDE, *p* = .0084; ED, *p* = .0065), 100 and 110 kV (CTDI, *p* = .0148; DLP, *p* = .0433; SSDE, *p* = .0350; ED, *p* = .0414), and 110 and 120 kV (CTDI, *p* = .0020; DLP, *p* = .0010; SSDE, *p* = .0123; ED, *p* = .0216).

Objective image quality analysis

Results of quantitative image quality analysis are summarized in Table 3 and shown in Fig. 1. Attenuation decreased continuously from 70 to 120 kV with significant differences for 70 vs. ≥80 kV (70 vs. 80 kV: proximal, *p* = .0080 and distal, *p* = .0148; 70 vs. 90, 100, 110 or 120 kV: proximal and distal, *p* < .0001, respectively), 80 vs. ≥100 kV (80 vs. 100 kV: proximal, *p* = .0003; distal, *p* = .0006; 80 vs. 110 kV: proximal, *p* = .0007 and distal, *p* = .0004; 80 vs. 120 kV: proximal and distal, *p* < .0001, respectively), 90 vs. ≥110 kV (90 vs. 110 kV: proximal, *p* = .0291 and distal, *p* = .0433; 90 vs. 120 kV: proximal and distal, *p* < .0001), and 100 vs. 120 kV (proximal, *p* = .0101; distal, *p* = .0023).

Image noise decreased continuously from 70 to 120 kV with significant differences noted between 70 and ≥90 kV (70 vs. 90 kV, *p* = .0007; 70 vs. 100, 110 or 120 kV, *p* < .0001, respectively), 80 and ≥90 kV (80 vs. 90 kV, *p* = .0238; 80 vs. 100 kV, *p* = .0002; 80 vs. 110 and 120 kV, *p* < .0001, respectively), and between 90 and ≥100 kV (90 vs. 100 kV, *p* = .0256; 90 vs. 110 or 120 kV, *p* < .0001, respectively).

Comparing SNR and CNR of studies at different tube voltages against each other did not reveal any significant differences for proximal SNR (*p*-values between .0829 and .8589), distal SNR (*p*-values between .0945 and .9752), proximal

Table 1 Patient characteristics

	70 kV	80 kV	90 kV	100 kV	110 kV	120 kV
No. of patients	43	39	37	40	23	90
Gender (male/female)	23/20	22/17	22/25	17/23	13/10	37/53
Body mass index in kg/m ² (95 % CI)	23.5 ± 3.3 (22.5-24.5)	26.6 ± 4.1 (25.2-28.0)*	27.1 ± 4.0 (25.7-28.5)	29.9 ± 4.5 (27.9-31.9)*	30.6 ± 4.4 (28.1-32.1)	34.4 ± 8.0 (32.6-36.1)*
Effective chest diameter in cm (95 % CI)	28.4 ± 2.0 (27.7-29.0)	29.8 ± 2.0 (29.2-30.5)*	30.9 ± 2.4 (30.1-31.7)*	31.5 ± 2.6 (30.6-32.3)	32.1 ± 2.9 (30.6-33.6)	34.4 ± 4.0 (33.5-35.3)*
Heart rate in beats per minute	68.1 ± 18.4	70.1 ± 13.6	64.1 ± 14.5	70.1 ± 16.1	67.6 ± 15.7	69.9 ± 10.3

CI: Confidence interval * indicates statistical significance between each 10 kV increment

Table 2 Radiation dose estimates

	70 kV	80 kV	90 kV	100 kV	110 kV	120 kV
No. of patients	43	39	37	40	23	90
Volume CT dose index in mGy	7.3 ± 5.7	11.3 ± 6.2*	14.8 ± 7.9*	21.8 ± 12.9*	26.3 ± 13.7*	37.2 ± 12.0*
Dose-length-product in mGy*cm	110.5 ± 86.5	174.5 ± 110.5*	244.3 ± 115.9*	421.5 ± 289.1*	595.6 ± 301.4*	767.8 ± 290.5*
Effective dose in mSv	1.5 ± 1.2	2.4 ± 1.5*	3.6 ± 2.7*	5.9 ± 4.0*	7.9 ± 4.2*	10.7 ± 4.1*
Size-specific dose estimates in mGy	9.4 ± 7.0	14.1 ± 8.0*	17.4 ± 7.6*	25.5 ± 15.1*	31.1 ± 15.9*	40.3 ± 12.7

* indicates statistical significance between each 10 kV increment

CNR (p -values between .2108 and .9920), or distal CNR (p -values between .2079 and .9988). Exact p -values are summarized in Supplementary Table 1.

Subjective image quality analysis

Detailed results of the subjective image quality analysis are summarized in Table 4 and Supplementary Table 2. Case examples are shown in Fig. 2.

Image quality was considered sufficient for diagnosis by observers in 98.9 % of the examinations on a per-patient basis. Two examinations (120 kV, BMI of 41.3 and 43.5 kg/m²) were considered suboptimal due to major image noise. Additionally, in one examination distal attenuation was rated as suboptimal (70 kV, BMI of 22.3 kg/m²), resulting in limited diagnostic confidence (score of 2).

Mean subjective image quality was rated good to excellent for both coronary artery attenuation and image noise at all tube voltages without significant differences for proximal and distal attenuation (p -values between .0840 and .9133 for proximal attenuation and between .0516 and .8590 for distal attenuation). However, image noise was rated as significantly higher for 70 kV studies when compared to CTA performed at ≥100 kV (70 vs. 100 kV, p = .0266; 70 vs. 110 kV, p = .0204 and 70 vs. 120 kV, p = .0143).

Good to excellent inter-observer agreement was achieved for vascular attenuation and image noise (κ range, 0.686–0.889, Supplementary Table 3).

Tube voltage selection and BMI/effective chest diameter

Increased patient BMI levels correlated with increased selected tube voltages from 70 to 120 kV for all 10 kV increments. Significant differences were observed between 70 and 80 kV (p = .0081), 90 and 100 kV (p = .0242), and 110 and 120 kV (p = .0453). No significant differences were found for 80 vs. 90 kV (p = .6136) or 100 vs. 110 kV (p = .6756).

In addition, increased effective chest diameter values also paralleled continuous increases in tube voltages ranging from 70 to 120 kV, noting significant differences between 70 and 80 kV (p = .0016), 80 and 90 kV (p = .0433), and also 110 and 120 kV (p = .0259). No significant differences were found for 90 vs. 100 kV (p = .3362) or 100 vs. 110 kV (p = .8238).

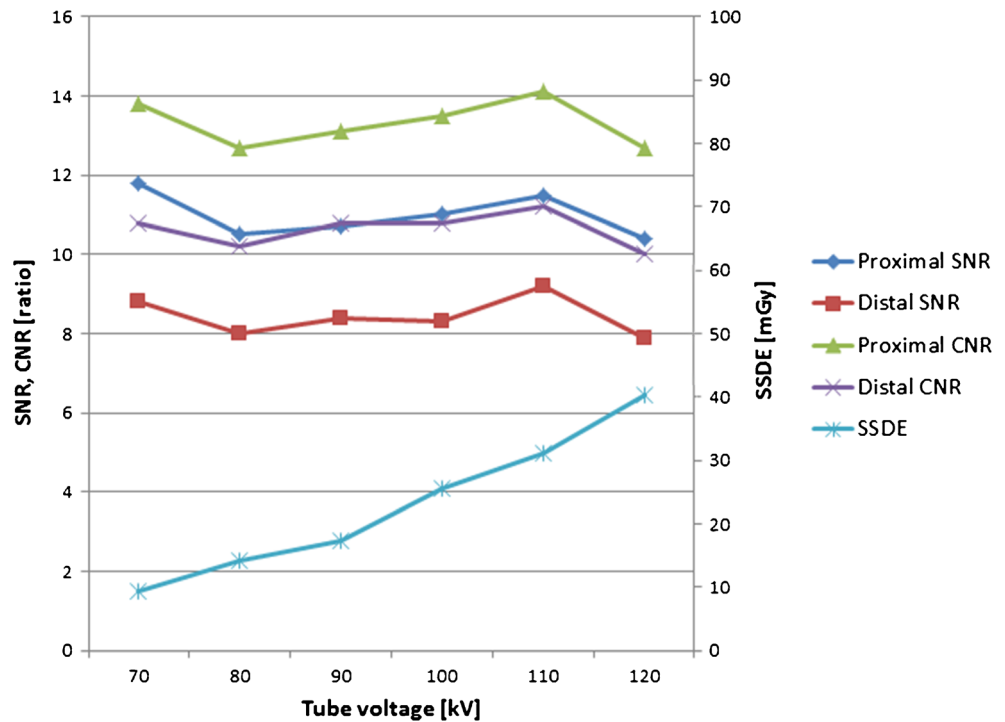
Spearman's correlation coefficient showed a positive association between effective chest diameter and BMI (ρ = .836; 95 % CI, .790 to .867; p = .0001), selected tube voltage and BMI (ρ = .639; 95 % CI, .590 to .702; p < .0001), and also tube voltage and effective chest diameter (ρ = .595; 95 % CI, .509 to .670; p < .0001; Fig. 3).

Table 3 Comparisons between objective image quality parameters

	70 kV	80 kV	90 kV	100 kV	110 kV	120 kV
Proximal attenuation in Hounsfield units	524.9 ± 150.4	441.8 ± 112.7	393.2 ± 95.3	352.5 ± 82.0	334.8 ± 80.2	310.4 ± 80.6
Distal attenuation in Hounsfield units	392.7 ± 116.4	333.8 ± 87.2	306.9 ± 77.4	285.9 ± 70.2	269.3 ± 57.4	229.3 ± 64.0
Image noise in Hounsfield units	47.8 ± 13.0	45.4 ± 14.5	38.9 ± 8.8	34.3 ± 8.3	30.4 ± 5.9	32.9 ± 10.7
Signal-to-noise ratio proximal	11.8 ± 5.1	10.5 ± 3.6	10.7 ± 3.9	11.0 ± 3.8	11.5 ± 4.0	10.4 ± 4.1
Signal-to-noise ratio distal	8.8 ± 3.5	8.0 ± 2.8	8.4 ± 3.3	8.3 ± 2.7	9.2 ± 2.9	7.9 ± 2.9
Contrast-to-noise ratio proximal	13.8 ± 5.5	12.7 ± 4.0	13.1 ± 4.5	13.5 ± 4.5	14.1 ± 4.1	12.7 ± 4.5
Contrast-to-noise ratio distal	10.8 ± 3.9	10.2 ± 3.3	10.8 ± 3.9	10.8 ± 3.3	11.2 ± 2.6	10.0 ± 3.3

Mean values and standard deviation of all measurements from left main, left anterior descending, circumflex, and right coronary artery

Fig. 1 Graph shows comparison between objective image quality and radiation dose at each tube voltage level. Stable image quality without significant differences is seen between the different tube voltages. Furthermore, a linear decrease was observed in size specific dose estimates towards lower tube voltages SNR, Signal-to-noise ratio; CNR, Contrast-to-noise ratio; SSDE, size-specific dose estimates



Discussion

Our results demonstrate that using ATVS for CCTA studies performed with a third generation DSCT system facilitates automated individual adaptation of tube voltages and determination of optimal examination parameters in clinical routine over a wide range of different patient sizes. The selection of low tube voltages significantly reduced radiation dose, yet still maintained image quality. Furthermore, our results showed that contrast medium volume can be adjusted based on tube voltage selection, reducing contrast medium requirements, while still providing intravascular attenuation sufficient for diagnosis. Previous studies have compared the use of AVTS to BMI-based tube voltage selections [12, 14], to standard 120 kV acquisitions [8-10; 13], and to the second generation DSCT AVTS algorithm, which allowed for tube voltage selection of 20 kV increments ranging between 80 and 140 kV [7]. AVTS has been recognized as an effective technique for radiation dose reduction; however, in these prior studies,

image quality of low-kV examinations was only compared with the reference standard. In contrast, we directly compared all selected tube voltages showing that image quality remains consistently high in the majority of examinations. Image quality was not acceptable for diagnosis in only two 120 kV studies and one 70 kV CCTA study (1.1 %).

Several technical improvements in the third generation DSCT system have created the potential to achieve image quality sufficient for diagnosis while still lowering tube voltage. New x-ray tubes in this system provide greater power reserves. The greater tube power mitigates previous tube current limitations at lower kV and makes low-kV imaging feasible for a broader patient population. In addition, a fully integrated circuit detector [23] and an advanced iterative reconstruction algorithm allow for enhanced image quality [5, 24–27].

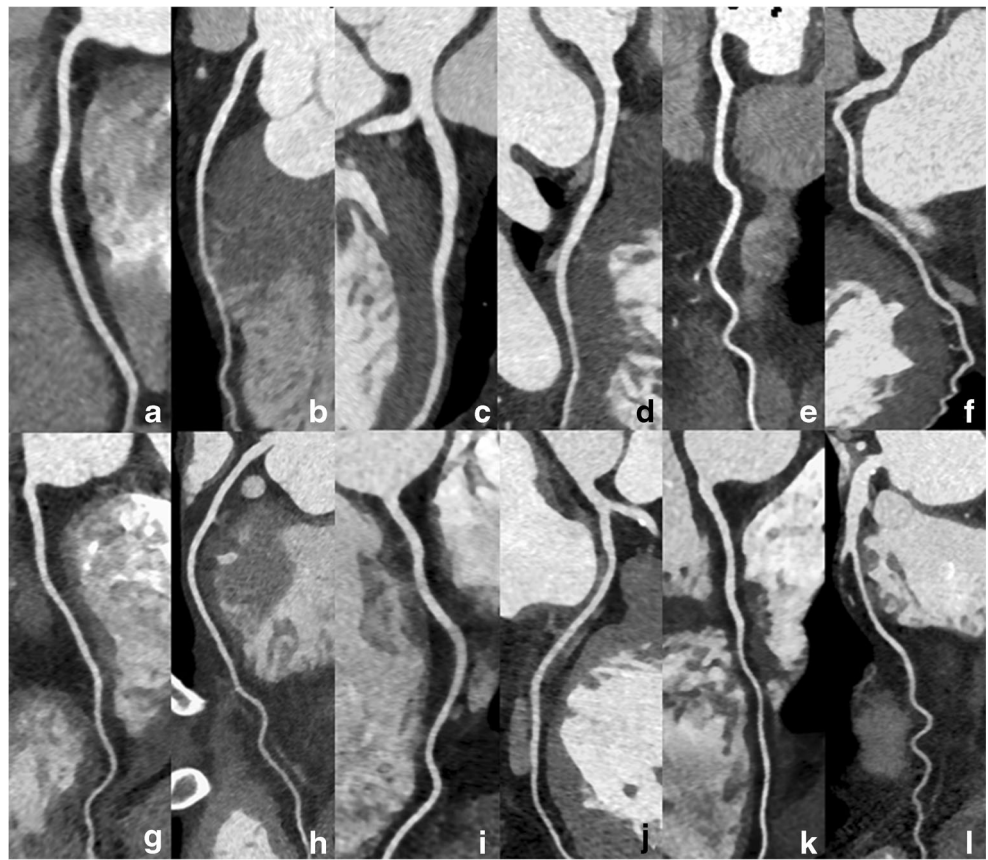
Along with tube voltage reductions, a continuous decrease in radiation dose was observed, resulting in a reduction of 86 % for ED between 120 kV and 70 kV studies based on

Table 4 Subjective image quality analysis

	70 kV	80 kV	90 kV	100 kV	110 kV	120 kV
Proximal attenuation	5.0 (5.0-5.0)	5.0 (5.0-5.0)	5.0 (4.5-5.0)	5.0 (4.5-5.0)	5.0 (5.0-5.0)	5.0 (4.0-5.0)
Distal attenuation	5.0 (4.0-5.0)	5.0 (4.0-5.0)	4.5 (4.0-5.0)	4.0 (4.0 – 5.0)	4.75 (4.0-5.0)	4.5 (4.0-5.0)
Image noise	4.0 (4.0-5.0)	5.0 (4.0-5.0)	5.0 (4.0-5.0)	5.0 (4.0-5.0)	5.0 (4.5-5.0)	4.5 (4.0-5.0)

Values are given for the median; interquartile range is shown in parentheses

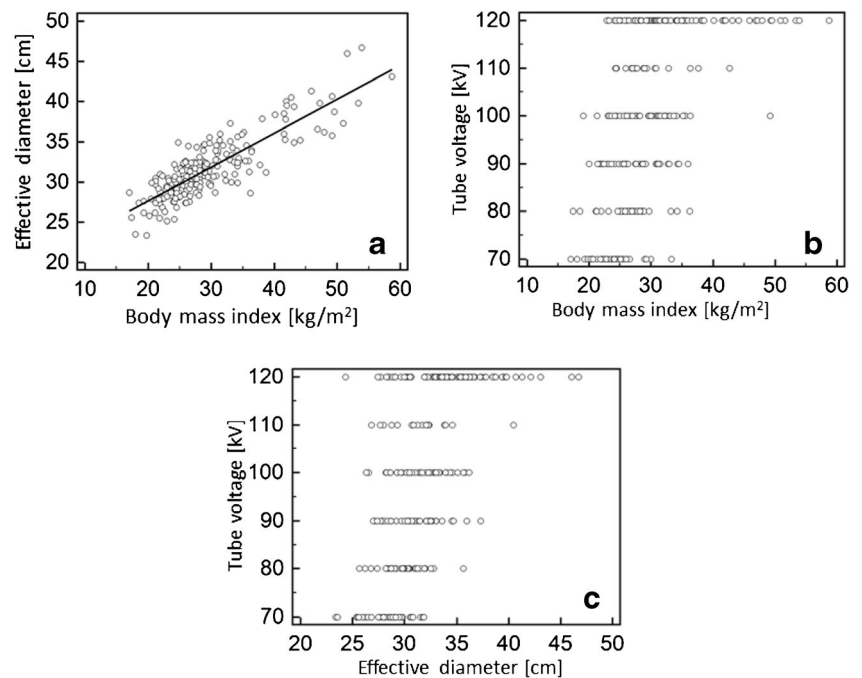
Fig. 2 Curved, multiplanar reformations of two exemplary coronary arteries from coronary CT angiography performed with tube voltages of 70 kV (**A** and **B**), 80 kV (**C** and **D**), 90 kV (**E** and **F**), 100 kV (**G** and **H**), 110 kV (**I** and **J**), and 120 kV (**K** and **L**) showing excellent vessel attenuation and no perceivable or minor image noise at each tube voltage. Image quality was rated as sufficient for diagnosis in all of these cases



CTDI_{vol} for a standardized 32 cm phantom. Since we included a wide range of patient body sizes, SSDE were used to compensate for inaccuracies in dose values for patient sizes

deviating from this phantom. We observed a reduction of 76.7 % for this same comparison, which can be explained by the smaller patient cohorts in low kV studies.

Fig. 3 Graphs show distribution of effective chest diameter plotted against body mass index (BMI, **A**), and tube voltage plotted against BMI (**B**) and effective diameter (**C**), respectively. A positive association was observed between effective diameter and BMI ($r = .836$), as well as tube voltage and BMI ($r = .639$) and effective diameter ($r = .585$), respectively



Several low-kV CTA studies have previously demonstrated good image quality with reduced contrast medium volume due to increased iodine attenuation [1, 3, 4]. However, to our knowledge, no prior studies have investigated ATVS vis-a-vis contrast medium reduction. In our study, we adjusted the contrast medium amount to the tube voltage and obtained intravascular attenuation sufficient for diagnosis in 99.6 % of CCTA studies. Suboptimal distal attenuation was observed in only one case (70 kV, BMI 22.3 kg/m²). The tube voltage reduction from ≥ 100 to 70 kV enabled a contrast medium reduction of 37.5 %. These results demonstrate that ATVS is an effective tool for both radiation dose and contrast medium reduction.

ATVS is a fully-automated algorithm that adjusts tube voltages not only to patient size, but also according to a combination of an individual patient's attenuation profile determined by the scout image, information on patient habitus, and the type of examination [7, 15]. This may explain why plotting BMI and effective chest diameter against tube voltage only showed a moderately positive correlation. However, mean BMI and effective diameter, which are commonly used for calculating SSDE [22, 28], showed a continuous increase from 70 kV to 120 kV. A stronger correlation was found for tube voltage and BMI than for tube voltage and effective diameter. Using these results, coupled with the fact that BMI values can usually be obtained more simply than effective diameter, we suggest using the proposed BMI thresholds to define an appropriate tube voltage if ATVS is not available. In this study, we did not increase tube voltages above 120 kV even in morbidly obese patients, even though higher tube voltages have been proposed for CCTA in obese patients [29, 30].

We acknowledge that this study has several limitations. First, we did not compare the diagnostic performance of CCTA versus invasive catheter angiography to detect significant coronary artery stenosis. Second, our results are currently only valid for third generation DSCT with the dose reduction techniques. Third, gender composition between groups was inhomogeneous, showing possible influences of breast tissue attenuation on the acquisition settings. Lastly, a fixed contrast agent volume was arbitrarily chosen for each kV level. Further investigations are necessary to more systematically define optimal contrast medium volumes for low-kV CCTA studies.

In conclusion, our results demonstrate that ATVS is an efficient algorithm facilitating individual tube-voltage adaptation at CCTA resulting in significantly reduced radiation dose while maintaining image quality. In addition, contrast medium volumes can be adjusted according to the automatically selected tube voltage, reducing contrast medium requirements at low-kV studies.

Acknowledgments The scientific guarantor of this publication is Prof. Dr. U. Joseph Schoepf. The authors of this manuscript declare

relationships with the following companies: Dr. Schoepf is a consultant for and receives research support from Astellas, Bayer, Bracco, GE, Medrad, and Siemens. Mr. Canstein is a Siemens employee. The other authors of this manuscript declare no relationships with any companies, whose products or services may be related to the subject matter of the article. The authors state that this work has not received any funding. One of the authors has significant statistical expertise. Institutional Review Board approval was obtained. Written informed consent was waived by the Institutional Review Board. The comprehensive results of automated tube voltage selection presented in this manuscript have not been reported yet. A fraction of the patients in this current study examined at 120 kV were included in a manuscript with a focus on cardiac imaging in morbidly obese patients which is currently under review at European Radiology (EURA-D-15-00876). Methodology: retrospective, cross-sectional, performed at one institution.

References

1. Meyer M, Haubenreisser H, Schoepf UJ et al (2014) Closing in on the K edge: coronary CT angiography at 100, 80, and 70 kV-initial comparison of a second- versus a third-generation dual-source CT system. *Radiology* 273:373–382
2. Zhang LJ, Zhao YE, Schoepf UJ et al (2015) Seventy-Peak Kilovoltage high-pitch thoracic aortic CT angiography without ECG gating: evaluation of image quality and radiation dose. *Acad Radiol* 22:890–897
3. Zhang LJ, Qi L, Wang J et al (2014) Feasibility of prospectively ECG-triggered high-pitch coronary CT angiography with 30 mL iodinated contrast agent at 70 kVp: initial experience. *Eur Radiol* 24:1537–1546
4. Lu GM, Luo S, Meinel FG et al (2014) High-pitch computed tomography pulmonary angiography with iterative reconstruction at 80 kVp and 20 mL contrast agent volume. *Eur Radiol* 24:3260–3268
5. Hell MM, Bittner D, Schuhbaeck A et al (2014) Prospectively ECG-triggered high-pitch coronary angiography with third-generation dual-source CT at 70 kVp tube voltage: feasibility, image quality, radiation dose, and effect of iterative reconstruction. *J Cardiovasc Comput Tomogr* 8:418–425
6. Hu L, Wang Y, Hou H, Wei F, Yang G, Chen Y (2014) Radiation dose and image quality with abdominal computed tomography with automated dose-optimized tube voltage selection. *J Int Med Res* 42: 1011–1017
7. Winklehner A, Gordic S, Lauk E et al (2015) Automated attenuation-based tube voltage selection for body CTA: performance evaluation of 192-slice dual-source CT. *Eur Radiol* 25: 2346–2353
8. Winklehner A, Goetti R, Baummueller S et al (2011) Automated attenuation-based tube potential selection for thoracoabdominal computed tomography angiography: improved dose effectiveness. *Invest Radiol* 46:767–773
9. Goetti R, Winklehner A, Gordic S et al (2012) Automated attenuation-based kilovoltage selection: preliminary observations in patients after endovascular aneurysm repair of the abdominal aorta. *AJR Am J Roentgenol* 199:W380–385
10. Siegel MJ, Ramirez-Giraldo JC, Hildebolt C, Bradley D, Schmidt B (2013) Automated low-kilovoltage selection in pediatric computed tomography angiography: phantom study evaluating effects on radiation dose and image quality. *Invest Radiol* 48:584–589

11. Schwarz F, Grandl K, Arnoldi A et al (2013) Lowering radiation exposure in CT angiography using automated tube potential selection and optimized iodine delivery rate. *AJR Am J Roentgenol* 200: W628–634
12. Layritz C, Muschiol G, Flohr T et al (2013) Automated attenuation-based selection of tube voltage and tube current for coronary CT angiography: reduction of radiation exposure versus a BMI-based strategy with an expert investigator. *J Cardiovasc Comput Tomogr* 7:303–310
13. Lurz M, Lell MM, Wuest W et al (2015) Automated tube voltage selection in thoracoabdominal computed tomography at high pitch using a third-generation dual-source scanner: image quality and radiation dose performance. *Invest Radiol* 50: 352–360
14. Krazinski AW, Meinel FG, Schoepf UJ et al (2014) Reduced radiation dose and improved image quality at cardiovascular CT angiography by automated attenuation-based tube voltage selection: intra-individual comparison. *Eur Radiol* 24:2677–2684
15. Spearman JV, Schoepf UJ, Rottenkolber M et al (2015) Effect of automated attenuation-based tube voltage selection on radiation dose at CT: an observational study on a global scale. *radiology*
16. Meinel FG, Canstein C, Schoepf UJ et al (2014) Image quality and radiation dose of low tube voltage 3rd generation dual-source coronary CT angiography in obese patients: a phantom study. *Eur Radiol* 24:1643–1650
17. Austen WG, Edwards JE, Frye RL et al (1975) A reporting system on patients evaluated for coronary artery disease. Report of the Ad Hoc Committee for Grading of Coronary Artery Disease, Council on Cardiovascular Surgery, American Heart Association. *Circulation* 51:5–40
18. Szucs-Farkas Z, Strautz T, Patak MA, Kurmann L, Vock P, Schindera ST (2009) Is body weight the most appropriate criterion to select patients eligible for low-dose pulmonary CT angiography? Analysis of objective and subjective image quality at 80 kVp in 100 patients. *Eur Radiol* 19:1914–1922
19. Yuan R, Shuman WP, Earls JP et al (2012) Reduced iodine load at CT pulmonary angiography with dual-energy monochromatic imaging: comparison with standard CT pulmonary angiography—a prospective randomized trial. *Radiology* 262:290–297
20. Christner JA, Braun NN, Jacobsen MC, Carter RE, Kofler JM, McCollough CH (2012) Size-specific dose estimates for adult patients at CT of the torso. *Radiology* 265:841–847
21. Deak PD, Smal Y, Kalender WA (2010) Multisection CT protocols: sex- and age-specific conversion factors used to determine effective dose from dose-length product. *Radiology* 257: 158–166
22. Boone JM SK, Cody DD, McCollough CH, McNitt-Gray MF, Toth TL (2011) Size-specific Dose Estimates (SSDE) in Pediatric and Adult Body CT Examinations. Report of Am Assoc Phys Med AAPM Task Group 204 2011 College Park, Md: American Association of Physicists in Medicine
23. Geyer LL, Glenn GR, De Cecco CN et al (2015) CT evaluation of small-diameter coronary artery stents: effect of an integrated circuit detector with iterative reconstruction. *Radiology* 276:706–714
24. Wang R, Schoepf UJ, Wu R et al (2012) Image quality and radiation dose of low dose coronary CT angiography in obese patients: sinogram affirmed iterative reconstruction versus filtered back projection. *Eur J Radiol* 81:3141–3145
25. Wang R, Schoepf UJ, Wu R et al (2014) Diagnostic accuracy of coronary CT angiography: comparison of filtered back projection and iterative reconstruction with different strengths. *J Comput Assist Tomogr* 38:179–184
26. Moscariello A, Takx RA, Schoepf UJ et al (2011) Coronary CT angiography: image quality, diagnostic accuracy, and potential for radiation dose reduction using a novel iterative image reconstruction technique-comparison with traditional filtered back projection. *Eur Radiol* 21:2130–2138
27. Gordic S, Desbiolles L, Stolzmann P et al (2014) Advanced modelled iterative reconstruction for abdominal CT: qualitative and quantitative evaluation. *Clin Radiol* 69:e497–504
28. Moore BM, Brady SL, Mirro AE, Kaufman RA (2014) Size-specific dose estimate (SSDE) provides a simple method to calculate organ dose for pediatric CT examinations. *Med Phys* 41: 071917
29. Leschka S, Stinn B, Schmid F et al (2009) Dual source CT coronary angiography in severely obese patients: trading off temporal resolution and image noise. *Invest Radiol* 44:720–727
30. Lee AM, Engel LC, Hui GC et al (2014) Coronary computed tomography angiography at 140 kV versus 120 kV: assessment of image quality and radiation exposure in overweight and moderately obese patients. *Acta Radiol* 55:554–562